

Fluorescence enabled Raman amplification using photonic crystal resonant modes

Cite as: Appl. Phys. Lett. **127**, 181104 (2025); doi: [10.1063/5.0295522](https://doi.org/10.1063/5.0295522)

Submitted: 9 August 2025 · Accepted: 16 October 2025 ·

Published Online: 6 November 2025



View Online



Export Citation



CrossMark

Fatma Uysal Ciloglu,^{1,2}  Seemesh Bhaskar,^{1,3,4}  Leyang Liu,^{1,3}  and Brian T. Cunningham^{1,3,4,5,6,7,a)} 

AFFILIATIONS

¹Nick Holonyak Jr. Micro and Nanotechnology Laboratory, University of Illinois at Urbana-Champaign, Urbana, Illinois 61801, USA

²Department of Biomedical Engineering, Erciyes University, Kayseri 38039, Türkiye

³Department of Electrical and Computer Engineering, University of Illinois at Urbana-Champaign, Urbana, Illinois 61801, USA

⁴Carl R. Woese Institute for Genomic Biology, University of Illinois at Urbana-Champaign, Urbana, Illinois 61801, USA

⁵Department of Bioengineering, University of Illinois at Urbana-Champaign, Urbana, Illinois 61801, USA

⁶Department of Chemistry, University of Illinois at Urbana-Champaign, Urbana, Illinois 61801, USA

⁷Cancer Center at Illinois, Urbana, Illinois 61801, USA

^{a)} Author to whom correspondence should be addressed: bcunning@illinois.edu

ABSTRACT

Although plasmonic and photonic crystal substrates represent fertile ground for plasmon-enhanced fluorescence, Raman scattering, and surface-enhanced Raman scattering based diagnostic tool development, extracting quantifiable Raman information from strongly fluorescent analytes without photobleaching, signal gating, or multi-step sample preparation has remained a long-standing challenge. In this work, we introduce Fluorescence Enabled Raman Amplification (FERA) as a mechanism that triggers the resonances of a photonic crystal surface and plasmonic nanoparticles via the molecular emission of a fluorescence-emitting radiating dipole, which, in turn, feeds back into molecular Raman scattering of the same molecules. This self-reinforcing feedback mechanism of FERA is experimentally demonstrated using multiple lasers and objectives and validated through COMSOL Multiphysics simulations. While the mesoscopic engineering presented valuable insights toward the generation of intense photonic-plasmonic hotspots, the microscopic engineering demonstrates the functionality of the radiating dipole as a dynamic entity with tailorable electronic and vibrational energy levels. By offering a simple, scalable, and label-compatible approach to photonic crystal-enhanced fluorescence in the transmittance mode and FERA in the reflectance mode, our study represents a pathway in the design of multifunctional plasmonic-photonic substrates and invites further exploration into light-matter interactions at the nanoscale.

Published under an exclusive license by AIP Publishing. <https://doi.org/10.1063/5.0295522>

Photonic crystal (PC)-based spectroscopic and microscopic technologies have significantly advanced the point-of-care diagnostics landscape, enabling highly sensitive and label-free detection mechanisms.^{1–3} Metal-free or plasmon-free high refractive index nanomaterials and other dielectric systems are being extensively studied for fluorescence^{2,4} and Raman spectroscopic and microscopic applications.^{5–8} Their integration with plasmonic structures enables further pushing the sensitivity boundaries for detecting low-abundance analytes, single molecules, or even subtle vibrational modes through enhanced Raman and fluorescence signals.^{8–10} In spite of these advancements, a long-standing challenge that has persisted over several years in the broad domain of photo-plasmonics is simultaneously augmenting both the fluorescence and Raman intensities of a given emitter.^{11–15} While Raman scattering yields exceptional chemical

specificity and vibrational resolution,^{5,14} fluorescence emission is regarded as an impediment especially in biological media because the broadband fluorescence emission often obscures the relatively weaker Raman modes.^{7,15,16} Particularly, since the Raman interrogation of emitters in visible or near-infrared regions is nearly impossible, substantial effort has been devoted to suppressing fluorescence using a variety of techniques including but not limited to instrumental gating and photobleaching protocols.^{13,17} However, it is worth noting that analytical methods focused on suppressing the fluorescence come at the cost of complex sample preparation introducing additional experimental steps.¹⁸ Although useful for certain applications, such a strategy is offset from the goal of harnessing every available photon.^{7,19,20}

With this background in mind, our approach is rooted in utilizing the fluorescence (rather than attempting to suppress it) where

engineering and coupling of fluorescence emission to optical resonances of a PC surface serves to amplify the Raman spectra of the same molecules. Through experimental measurements and simulations, we demonstrate the constructive integration of the PC-enhanced fluorescence excitation into the Raman enhancement process via a self-reinforcing mechanism. Extrapolating from the foundational “radiating plasmon” model introduced by Lakowicz²¹ and our recently developed radiating guided mode resonance (GMR) model,^{2,22,23} we report a PC-based internal optical feedback mechanism where the emitted photons from fluorescent emitters augment their own Raman signal. Hence, simultaneous enhancement of fluorescence and Raman signals is presented via a dual-mode PC response in transmission and reflection modes. The implications of this investigation extend beyond fundamental photo-plasmonics to practical applications, especially in scenarios where fluorescence and Raman signatures yield valuable insights of bioanalytes.

In principle, our system is designed to generate the GMR of the PC with the emitted photons from the fluorophore as shown in Fig. 1.

This results in directional (steered) and polarized emission carrying emission spectral feature in the transmittance mode (the details of which are presented in Fig. 2).² Consequently, upon excitation of the GMR, near-field intensity is observed sustaining electromagnetic standing waves with associated “hotspot” regions of enhanced electric field intensity.^{23,24} These hotspots, in turn, enhance the Raman vibrational modes of the same emitter molecule that initiated the process. As the concepts presented here with support from simulations introduce a paradigm, the interlinked excitation-emission loop, where the fluorescence augments its own Raman feature via GMR coupling, we introduce terminology for this effect: Fluorescence-Enabled Raman Amplification (FERA). Figure 1(b) shows the topographical 3D view of the PC interface. The absorption and emission spectra of the rhodamine B (RhB) emitter are shown in Fig. 1(c). The GMR resonances of the PC under white light excitation are shown in Fig. 1(d) along with the inset showing the highly uniform PC substrate (the details of fabrication and structural dimensions are presented in our recent works).^{2,7,10,23} The Raman spectra observed for 1 mM RhB

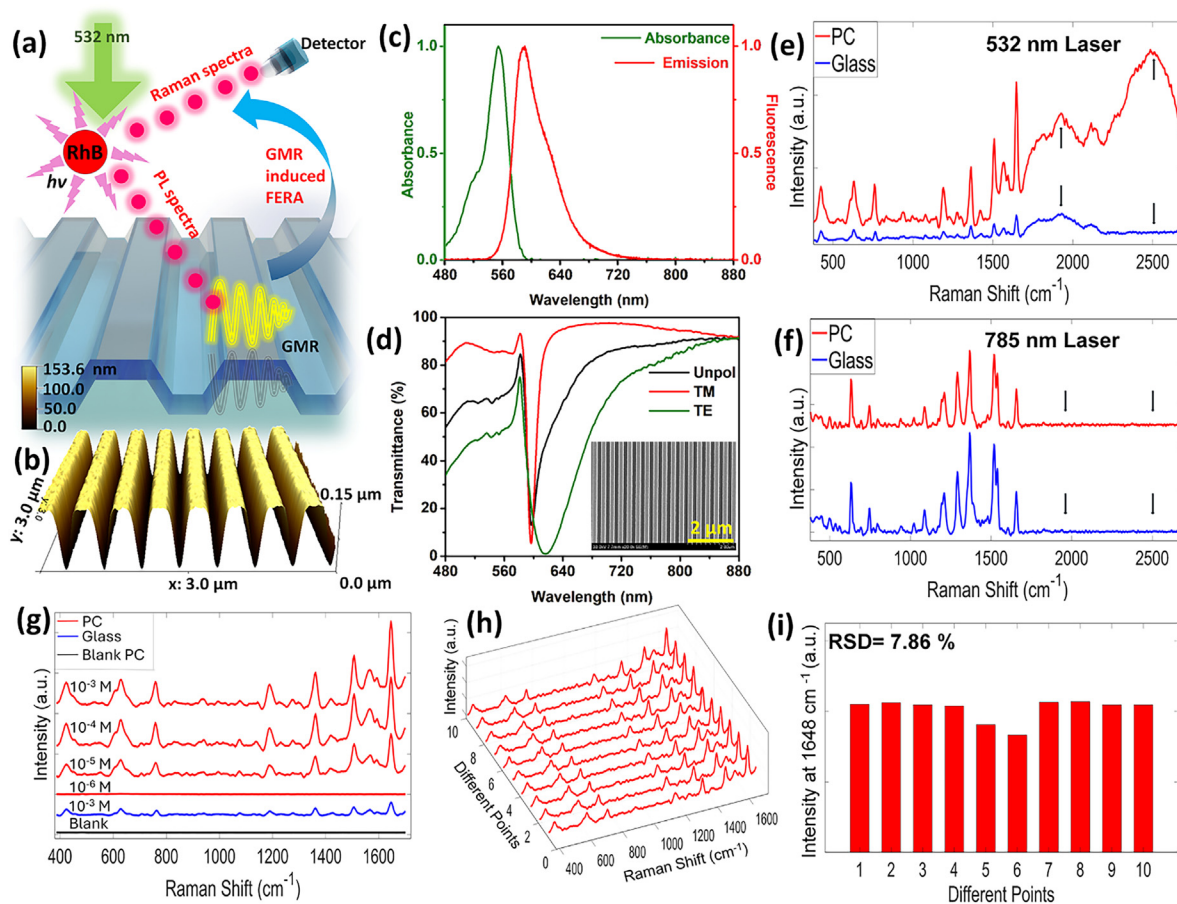


FIG. 1. Photonic crystal-enhanced Raman via fluorescence feedback in reflectance mode. (a) Conceptual illustration of the internal feedback mechanism where the emission from the radiating dipoles excites the GMR, which, in turn, enhances the Raman of the emitter. (b) 3D AFM height profile of the PC. (c) Absorbance and emission spectra of the RhB molecules. (d) Unpolarized, TE, and TM-polarized transmittance spectra of the PC shown with the top view as an SEM inset. Raman spectra of RhB on PC and glass excited with a (e) 532 nm and (f) 785 nm laser wavelength. (g) Raman spectra of RhB at varying concentrations on PC (from 10^{-3} to 10^{-6} M), compared with 10^{-3} M on glass. (h) Measurements of 10^{-4} M RhB on the PC at several locations. (i) The peak intensity changes of RhB for the 1648 cm^{-1} peak position measured at 10 different locations on the PC.

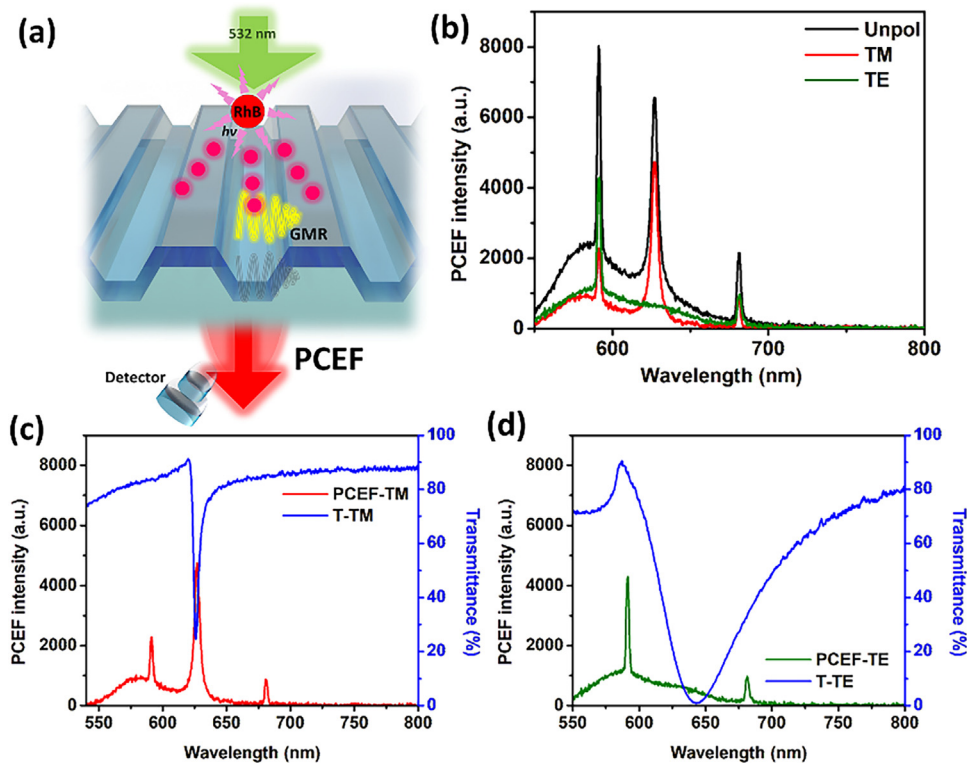


FIG. 2. Photonic crystal-enhanced fluorescence (PCEF) in transmittance mode. (a) Schematic illustration of the fluorescence emission steered by the PC interface upon GMR excitation. (b) PCEF spectra for unpolarized, TE, and TM-polarized emission. Overlap of the (c) TM and (d) TE polarized emission of RhB radiating dipoles with the transmittance response.

concentration (prepared by dropping and drying at room temperature) on glass and PC substrates obtained using 532 and 785 nm lasers are shown in Figs. 1(e) and 1(f), respectively. Analysis of these data indicates the occurrence of broad Raman shift spectra around 1800 and 2500 cm^{-1} , corresponding to wavelengths of 590 and 615 nm, respectively, for 532 nm laser excitation. The 590 nm (1800 cm^{-1}) spectra correspond well with the emission maximum of the RhB upon 532 nm excitation [Fig. 1(c)]. Importantly, the 615 nm (2500 cm^{-1}) spectra correspond to the wavelength where we observe the GMR of the PC. This observation corroborates well with the higher intensity of the GMR-enhanced fluorescence observed at 2500 cm^{-1} as compared to the pristine fluorescence of RhB (which corresponds to 1800 cm^{-1}). Moreover, the fluorescence of the RhB was not observed under 785 nm excitation wavelength as it does not overlap with the absorption spectra of the RhB. Hence, the total Raman output observed under 532 nm excitation is the result of enhanced excitation and enhanced emission of the radiating dipoles facilitated by the underlying PC.^{2,23} Furthermore, RhB Raman signals are detectable on the PC from concentrations extending from 10^{-3} M to 10^{-5} M [Fig. 1(g)]. Importantly, the Raman intensity on a glass substrate is significantly lower than that observed on the PC even at the highest concentration. Based on this comparison, the enhancement factor (EF) provided by the PC is calculated to be 6.63×10^2 using the following equation:

$$AEF = \frac{I_{SERS}/C_{SERS}}{I_{Raman}/C_{Raman}}. \quad (1)$$

Furthermore, the PC substrate demonstrates high uniformity [Fig. 1(h)] in Raman spectra collected from ten different locations. The

relative standard deviation (RSD) was calculated to evaluate signal repeatability. The spectra collected on the PC show only 7.68% deviation in peak intensity at 1648 cm^{-1} [Fig. 1(i)]. Incorporating two laser sources and careful analysis over the glass and PC substrates under identical conditions, these initial optimizations present encouraging results establishing the robustness of the FERA effect. The fluorescence emission spectra observed for the same substrate with the emission collected in the transmittance mode are presented in Fig. 2.

The fluorescence emission outcoupled from the PC surface into the far-field is collected using an optical fiber coupled to a spectrometer (Ocean Optics 2000+), in line with our earlier works.^{2,22,23} Upon 532 nm excitation, the emitted photons from the radiating dipoles carry the broad emission profile [seen in Fig. 1(c)] while striking the PC. Consequently, the GMR modes of the underlying PC are excited. Following this, the emission of the fluorophores travels to the far-field carrying the spectral signature of the RhB and the polarization selectivity of the underlying PC (Fig. 2).²⁵ Figure 2(b) presents unpolarized, TM, and TE polarized output of the emission, which is also overlapped with the respective TM and TE transmittance spectra in Figs. 2(c) and 2(d). This is analogous to the photonic crystal coupled emission (PCCE)²⁶ and surface plasmon-coupled emission (SPCE) technologies^{27,28} explored previously using Bragg mirror-based PCs and metal-dielectric interfaces. While these platforms need a prism to collect emitted photons, our PC channels emission directly into the far-field, aligning with our recently developed steering emission method.^{2,7,10,23} The characteristic properties of each of these modes are fully described in our recent works.^{2,22} In brief, while the TM coupled fluorescence overlaps well with the GMR of the PC [Fig. 2(c)], the TE coupled

emission shows extremely narrow coupling to the photonic band edge of the PC [Fig. 2(d)].²² Importantly, the fluorescence emission from the RhB radiating dipoles not only excites all the underlying modes of the PC but also travels to the far-field carrying the spectral feature of the emission, facilitating biosensing applications in transmittance mode. Simultaneously, the excited GMR further augments the Raman signature of the same fluorescent molecules in the reflectance mode similar to the typical surface-enhanced Raman scattering (SERS) phenomena.

To further enhance the Raman signal, we introduced metal nanoparticles to the system, with the goal of utilizing fluorescence emission for self-excitation of SERS. Originally, the radiating plasmon model introduced by Lakowicz and coworkers demonstrated a paradigm in understanding the functionality of an emitter coupled to a plasmonic entity (nanoparticle or thin film).^{21,27} Inspired by such reports, our group recently introduced a generalized radiating GMR model explaining the interplay between the spontaneous emission processes, lifetime engineering, and optical resonances in high-quality factor PC substrates, enabling pathways for modulating directionality and spectral features for ultra-sensitive biosensing.^{2,22,23} Moreover, we have shown that incorporating plasmonic nanomaterials sustaining localized surface plasmon resonance (LSPR) onto the PC results in the generation of hybridized modes at the intersection, where the emitter is located enhancing the photostability.^{7,8} In this background, the effects of LSPR- and GMR-enhanced Raman observed by interfacing the emitters on silver nanoparticles (AgNP) are schematically demonstrated in Fig. 3(a). The AFM 3D topographical image shows higher surface roughness when AgNPs are added at a density of $20.3 \times 10^6 \pm 1.59 \times 10^6$ particles/mm² [Fig. 3(b)]. The TEM image of the AgNP is shown along with its HRTEM image in Fig. 3(c) along with the lattice fringes corresponding to Ag (ICSD reference code: 98-005-3759; lattice parameters: $a = b = c = 4.0680 \text{ \AA}$, $\alpha = \beta = \gamma = 90^\circ$). The uniform distribution of AgNPs over the PC substrate is observed in the SEM image [Fig. 3(d)]. The methodology adopted for the generation

of the AgNPs over the PC substrate is detailed in the [supplementary material](#). In addition to comprehensive material and substrate characterization, we have also performed simulations to understand the near-field hotspot effects. Furthermore, the COMSOL simulations performed for the case of glass and PC substrates with and without AgNPs clearly indicate an enhancement in the near-field effects observed in the hybrid interface of PC+AgNPs.²⁹

The experimental results obtained using this hybrid AgNPs+PC interface are shown in Fig. 4(a), with SERS spectra collected with different concentrations of RhB. The synergistic effect of the LSPR from the AgNPs and the GMR from the PC further yields better enhancement factor, calculated as 1.94×10^6 . Moreover, SERS spectra of RhB obtained in the concentration range from $1 \mu\text{M}$ to 1 nM on the AgNP-coated PC surface reveal a clear linear relationship between the intensity of the characteristic peak at 1648 cm^{-1} and RhB concentration [Fig. 4(b)]. While the coefficient of determination value (R²) was found as 0.96, presenting an excellent fit of the model with the data, the linear relationship demonstrates the high reliability of the sensor performance at low concentration, which is suitable for quantitative SERS-based diagnostic platforms.

The rational design of promising biosensing frameworks based on fluorescence and Raman spectroscopy is grounded in understanding the mechanisms of light-matter interactions from three important perspectives, namely, (i) microscopic, (ii) mesoscopic, and (iii) macroscopic domains.^{20,30} Typically, the microscopic engineering comprises modulating the electronic and vibrational energy levels of the radiating dipoles by altering the local EM environment.^{23,31} Although the conventional fluorescence-based explorations treat a radiating dipole as a passive entity performing downconversion, our approach utilizes the emission of the dipole (following electronic excitation) to excite the GMR mode as well as the LSPR of the plasmonic NP [Fig. 3(a)], which, in turn, re-amplifies the Raman scattering vibrational modes of the same emitter, which is also a Raman reporter (RhB). This is

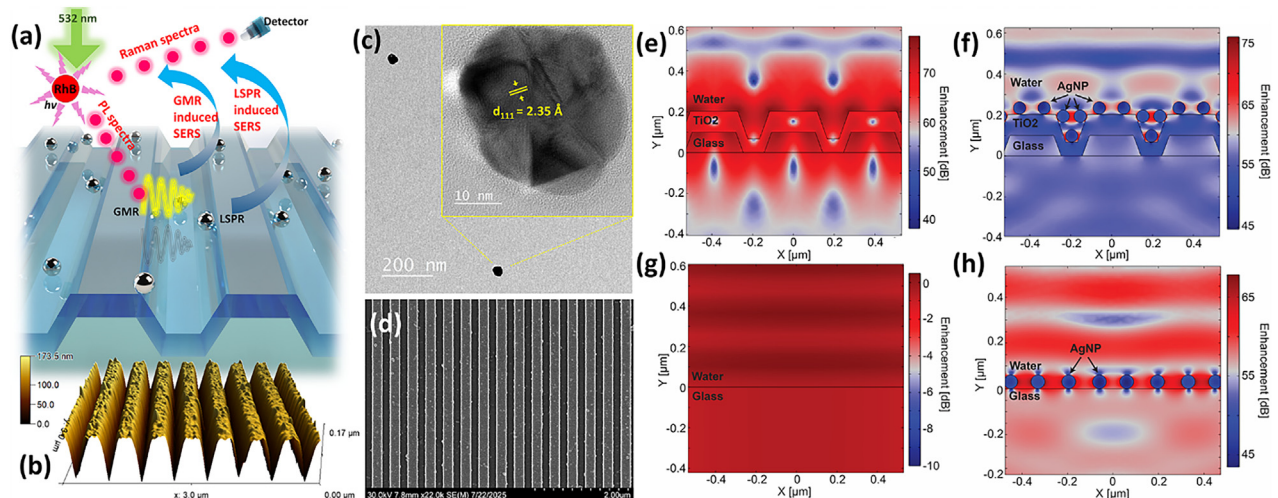


FIG. 3. Interfacing plasmonic AgNPs over PC for augmenting SERS. (a) Conceptual schematic showing the dual pathways augmenting the Raman spectra of RhB emitter via LSPR of AgNPs and GMR of PC. (b) 3D AFM view of the PC substrate decorated with AgNPs. (c) TEM image of the AgNPs with inset showing the HRTEM image presenting lattice fringes. (d) SEM image of the AgNPs decorating the PC substrate. COMSOL Multiphysics simulations of PC substrate (e) without and (f) with AgNPs and the same for glass substrate are shown in (g) and (h), respectively.

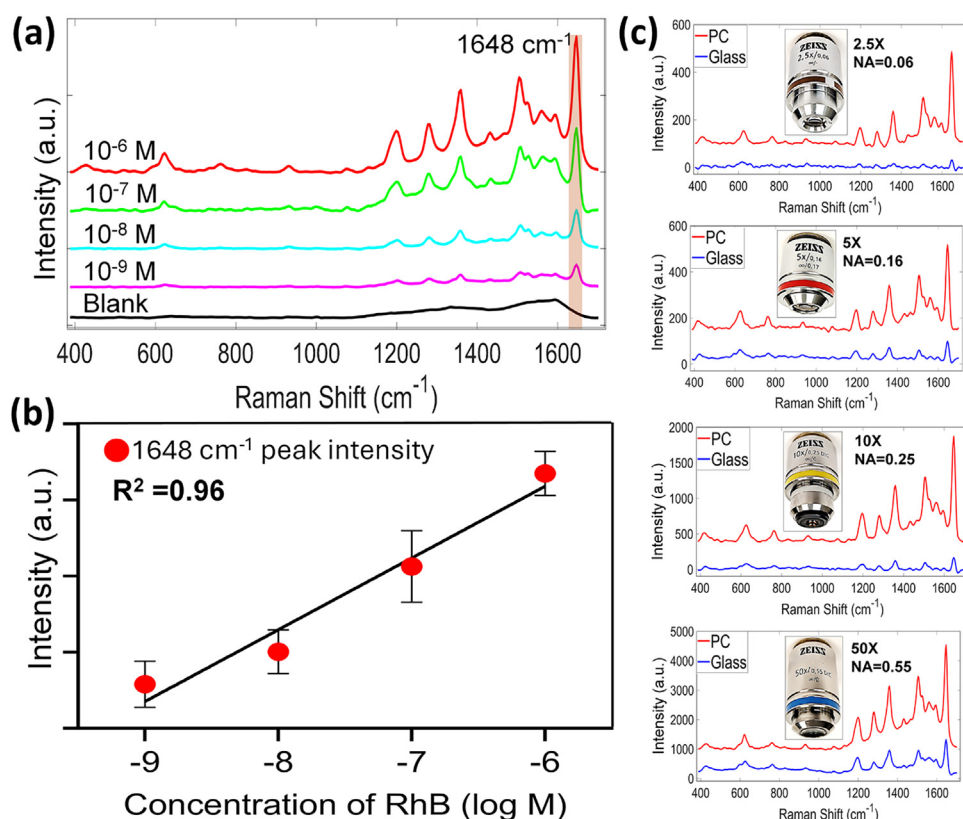


FIG. 4. Photonic crystal - Plasmonic hybrid interface for augmenting Raman intensity via FERA. (a) Raman spectra of RhB at different concentrations (from 10^{-6} to 10^{-9}) with AgNPs - PC hybrid interface. (b) Concentration-dependent SERS intensity of the 1648 cm^{-1} peak for RhB. (c) SERS signal intensity of RhB on AgNP-coated PC and glass surfaces collected using different objectives.

dramatically different from typical substrates where a variety of plasmonic NP configurations have been utilized for near-field hotspot generation. From a microscopic engineering point of view, the EM surroundings of the emitters are modified by their own electronic excitations, which, in turn, alters the molecules' scattering efficiency, hence representing the molecule as a dynamic entity (not a passive energy transformer), which renders nontrivial enhancements.^{2,31} Results associated with the lifetime engineering of such emitters near plasmonic and PC substrates from our recent works^{2,10} further re-iterate the mechanism, as this is accompanied by reduction of fluorescence lifetime, enhancement in quantum yield, and photostability, due to the cascading radiative decay rate on the account of synergistic effects of LSPR and GMR.

Furthermore, it is important to discuss the results captured in Figs. 4(a) and 4(b) by introducing the careful considerations of mesoscopic engineering aspects. By and large, the mesoscopic engineering is associated with two key aspects: (i) geometrical (structure-to-property relationship) and (ii) physico-chemical (dielectric function, resonance, and gain/loss) properties.^{7,23,31} Earlier works focused on the development of myriad local electric field amplifying approaches using sharp nano-micro-morphologies, nanotips, nano-crevices, and nanovoids to name a few, rendering the effects of tip-core plasmons, lightning rod effects, localized, delocalized, and propagating plasmons. In contrast, the synergistic approach of a plasmonic-PC resonator system to enhance the Raman scattering output of a fluorescent reporter via its own fluorescence is seldom explored.^{7,11,15} In this context, the PC is designed to sustain GMR so as to spectrally coincide with the emission

profile of the radiating dipole. This approach facilitates the excitation of GMR of the PC via the emitted photons from the radiating dipoles (in contrast to conventional systems, where excitation of GMR is necessary directly by the excitation laser).^{1,32} The hotspots that are, hence, generated at the PC interface perform two crucial roles in the presence of plasmonic AgNPs, namely, (i) they expedite the formation of hybrid metal (Ag)-dielectric (PC) hotspots, which, in turn, increase the scattering cross section of the Raman-active modes of the radiating dipoles. (ii) Stimulation of such hybrid resonances by the emission of the radiating dipole itself would introduce an altered feedback loop, where the emitter functions not just as an enhanced excitation source but also as a Raman probe in the hybrid Ag-PC hotspot. From a mesoscopic engineering standpoint, the spatial co-localization and the spectral overlap between the emission of the radiating dipoles, GMR of the PC, and the LSPR of the plasmonic AgNPs would render hybrid plasmonic-photonic coupling routes.

Furthermore, as the macroscopic engineering^{20,31} constitutes understanding the effects of optical elements such as objectives, mirrors, and lenses, we performed additional optimizations to understand the effect of SERS spectra of $1 \mu\text{M}$ RhB collected using 50 \times , 10 \times , 5 \times , and 2.5 \times objective lenses on both the AgNP-coated PC and AgNP-coated glass substrates (Fig. 4). As anticipated, SERS signal intensity decreases with decreasing magnification due to the lower numerical aperture and reduced light collection efficiency of low-power objectives. However, the decrease in signal intensity is significantly more prominent on the glass substrate as compared to the PC. Importantly, for the 2.5 \times magnification, while the SERS signal collected from RhB

on the PC substrate shows a high signal intensity ratio, the signal from the glass surface becomes barely detectable with poor spectral quality. These results highlight the ability of the AgNP-PC hybrid system to render dramatically higher SERS signals, even under low-magnification conditions, thereby emphasizing the robustness of the system toward minimizing the macroscopic components (such as additional light focusing optics).^{7,20} This is achievable, in principle, because of the intrinsic match between the GMR and emitter, thereby relying less on extraneous macroscopic optical components and enabling direct and easy-to-understand interpretation of the resonance-enhanced effects. Considering the high cost of high-magnification objectives, the ability to obtain high-quality Raman signals using a low-cost $2.5\times$ objective makes the PC substrate highly advantageous for sensing applications.

Although the current proof-of-concept demonstration utilizes Rhodamine B for simplicity, the underlying principle is broadly applicable to fluorescently tagged biomolecules widely used in biological and clinical assays. In this context, fluorescence becomes a functional handle rather than a limitation, enabling photonic crystal platforms to synergistically enhance both fluorescence and Raman signals. The structural tunability of PCs further allows tailoring of the GMRs to match specific fluorophore emission bands, thus extending this approach toward a wide class of analytes relevant for bioassays and molecular diagnostics.⁷

In summary, the vision of this work has been a departure from conventional goals of SERS, where instead of suppressing the emission,³³ we engineer the interface to leverage the emission of the radiating dipole to excite the Raman signal of the same emitter. While the enhanced fluorescence can be collected in the transmittance mode,^{2,10} the reflectance mode is utilized here to augment the Raman spectra, hence establishing a dual-mode sensing approach. The hybrid mode engineering with the self-reinforcing loop demonstrating augmented SERS presents far-reaching implications for bio-chemical analysis of target analytes, where instead of finding pathways to mitigate the fluorescence, our approach relies on using it as a source for symbiotically enhancing the resonance-driven plasmonic-photonic coupling effects.

See the [supplementary material](#) for information regarding synthesis and characterization of nanoparticles, PC structural details, APS functionalization and coating of AgNPs, overlap of the experimental transmittance of the PC with the PCEF obtained in the transmittance mode, and additional data from Raman and SERS measurements.

The authors gratefully acknowledge funding from the National Institutes of Health (R01AI159454, R01CA227699, R01AI139401, R01EB029805, and RadXRad Program Grant No. U01AA029348) and the National Science Foundation (NSF Nos. RAPID 20-27778, CBET 19-00277, and CBET 22-32681). Financial support was also provided by the Cancer Center at Illinois. F.U.C. is supported by the Scientific and Technological Research Council of Türkiye. S.B. is supported by Carl R. Woese Institute for Genomic Biology. The authors thank the research scientists Kathy Walsh, Ying He, Wacek Swiech, Honghui Zhou, and Julio Antonio Nieri D Soares for their support and research inputs in characterization of materials. The support from the instruments *Asylum Research MFP-3D AFM*, *Hitachi S-4800 High Resolution SEM*, *Au-Pd Sputter Coater - Emscope SC 500*, *FEI Helios 600i Dual Beam SEM/FIB*, and *JEOL*

2100 CRYO TEM, and the associated staff and research scientists at Materials Research Laboratory, The Grainger College of Engineering, UIUC, are gratefully acknowledged. The authors extend special thanks to the IGB state-of-the-art Core facilities. The Raman data presented in this work are collected at this core using *WITec Alpha 300 RA Raman-AFM-SNOM confocal Raman imaging system*. The support from research scientists at the core: Umnia Doha, Austin Cyphersmith, Duncan Nall, Miranda O'Dell, and Glenn Fried are gratefully acknowledged. The authors thank the feedback provided by all the members of the *Nanosensors* group, HMNTL, during scientific discussions.

AUTHOR DECLARATIONS

Conflict of Interest

The authors have no conflicts to disclose.

Author Contributions

Fatma Uysal Ciloglu and Seemesh Bhaskar contributed equally to this work.

Fatma Uysal Ciloglu: Conceptualization (lead); Data curation (lead); Formal analysis (lead); Funding acquisition (equal); Investigation (lead); Methodology (lead); Software (equal); Validation (equal); Visualization (lead); Writing – original draft (equal); Writing – review & editing (equal). **Seemesh Bhaskar:** Conceptualization (equal); Data curation (equal); Formal analysis (equal); Funding acquisition (equal); Investigation (equal); Methodology (equal); Software (equal); Validation (equal); Visualization (equal); Writing – original draft (equal); Writing – review & editing (equal). **Leyang Liu:** Data curation (equal); Formal analysis (supporting); Investigation (supporting); Methodology (supporting); Software (lead); Validation (supporting); Writing – original draft (supporting). **Brian T. Cunningham:** Conceptualization (equal); Project administration (equal); Resources (equal); Software (equal); Supervision (equal); Validation (equal); Visualization (equal); Writing – review & editing (equal).

DATA AVAILABILITY

The data that support the findings of this study are available from the corresponding author upon reasonable request.

REFERENCES

- ¹N. Ganesh, W. Zhang, P. C. Mathias, E. Chow, J. A. N. T. Soares, V. Malyarchuk, A. D. Smith, and B. T. Cunningham, *Nat. Nanotechnol.* **2**(8), 515 (2007).
- ²S. Bhaskar, W. Liu, J. Tibbs, and B. T. Cunningham, *Appl. Phys. Lett.* **124**(16), 161102 (2024).
- ³L. Liu, S. Bhaskar, and B. T. Cunningham, *Appl. Phys. Lett.* **124**(23), 234101 (2024); A. Pokhriyal, M. Lu, C. S. Huang, S. Schulz, and B. T. Cunningham, *Appl. Phys. Lett.* **97**(12), 121108 (2010); H. Inan, M. Poyraz, F. Inci, M. A. Lifson, M. Baday, B. T. Cunningham, and U. Demirci, *Chem. Soc. Rev.* **46**(2), 366 (2017).
- ⁴S. Bhaskar, N. S. Visweswar Kambhampati, K. M. Ganesh, P. M. Sharma, V. Srinivasan, and S. S. Ramamurthy, *ACS Appl. Mater. Interfaces* **13**(14), 17046 (2021).
- ⁵I. Alessandri, *J. Am. Chem. Soc.* **135**(15), 5541 (2013).
- ⁶I. Alessandri and J. R. Lombardi, *Chem. Rev.* **116**(24), 14921 (2016); N. Bontempi, I. Vassalini, and I. Alessandri, *J. Raman Spectrosc.* **49**(6), 943 (2018); S. Bhaskar, Y. Xiong, S. Shepherd, J. Tibbs, A. K. Bacon, W. Liu, L. D. Akin, T. Ayupova, W. Wang, H. Lee, L. Liu, A. Tan, K. Khemtonglang, X.

- Wang, and B. T. Cunningham, in *Nano-Engineering at Functional Interfaces for Multi-Disciplinary Applications* (Elsevier, 2025), p. 123; N. Bontempi, I. Vassalini, S. Danesi, M. Ferroni, M. Donarelli, P. Colombi, and I. Alessandri, *J. Phys. Chem. Lett.* **9**(9), 2127 (2018).
- ⁷S. Bhaskar, W. Wang, H. Lee, L. Liu, S. Umrao, W. Liu, A. Bacon, J. Tibbs, K. Khemtonglang, A. Tan, T. Ayupova, W.-C. Chen, X. Wang, and B. T. Cunningham, *Chem. Rev.* **125**(14), 6435–6540 (2025).
- ⁸S. Bhaskar, W. Liu, S. Shepherd, D. Wijewardena, J. Tibbs, and B. T. Cunningham, *Adv. Funct. Mater.* e12295 (2025).
- ⁹S. Shepherd, W. Liu, S. Bhaskar *et al.*, *Anal. Bioanal. Chem.* (2025); C. Che, R. Xue, N. Li, P. Gupta, X. Wang, B. Zhao, S. Singamaneni, S. Nie, and B. T. Cunningham, *ACS Nano* **16**(2), 2345 (2022).
- ¹⁰K. M. Ganesh, S. S. M. Lis, S. P. Nayak, P. Das, S. Bhaskar, N. Reddy, M. A. Hossain, C. B. Sanjeevi, S. S. Ramamurthy, and B. S. Bhaktha, "Surface plasmon resonance waveguides and their applications: Insights from functional metal-dielectric-metal interfaces," in *Nano-Engineering at Functional Interfaces for Multi-Disciplinary Applications* (Elsevier, 2025), pp. 93–121.
- ¹¹J. Langer, D. J. de Aberasturi, J. Aizpurua, R. A. Alvarez-Puebla, B. Augu  , J. J. Baumberg, G. C. Bazan, S. E. J. Bell, A. Boisen, A. G. Brolo, J. Choo, D. Cialla-May, V. Deckert, L. Fabris, K. Faulds, F. J. Garc  a de Abajo, R. Goodacre, D. Graham, A. J. Haes, C. L. Haynes, C. Huck, T. Itoh, M. K  ll, J. Kneipp, N. A. Kotov, H. Kuang, E. C. Le Ru, H. Kwee Lee, J.-F. Li, X. Yi Ling, S. A. Maier, T. Mayerh  fer, M. Moskovits, K. Murakoshi, J.-M. Nam, S. Nie, Y. Ozaki, I. Pastoriza-Santos, J. Perez-Juste, J. Popp, A. Pucci, S. Reich, B. Ren, G. C. Schatz, T. Shegai, S. Schl  cker, L.-L. Tay, K. G. Thomas, Z.-Q. Tian, R. P. Van Duyne, T. Vo-Dinh, Y. Wang, K. A. Willets, C. Xu, H. Xu, Y. Xu, Y. S. Yamamoto, B. Zhao, and L. M. Liz-Marz  n, *ACS Nano* **14**(1), 28 (2020).
- ¹²P. K. Badiya, S. G. Patnaik, V. Srinivasan, N. Reddy, C. S. Manohar, R. Vedarajan, N. Mastumi, S. K. Belliraj, and S. S. Ramamurthy, *Chem. Phys. Lett.* **685**, 139 (2017); M. Li, S. K. Cushing, and N. Wu, *Analyst* **140**(2), 386 (2014); F. Zou, H. Zhou, T. V. Tan, J. Kim, K. Koh, and J. Lee, *ACS Appl. Mater. Interfaces* **7**(22), 12168 (2015).
- ¹³M. K  ll, H. Xu, and P. Johansson, *J. Raman Spectrosc.* **36**(6–7), 510 (2005).
- ¹⁴N. Bontempi, L. Carletti, C. De Angelis, and I. Alessandri, *Nanoscale* **8**(6), 3226 (2016).
- ¹⁵J. Yi, E.-M. You, R. Hu, D.-Y. Wu, G.-K. Liu, Z.-L. Yang, H. Zhang, Y. Gu, Y.-H. Wang, X. Wang, H. Ma, Y. Yang, J.-Y. Liu, F. R. Fan, C. Zhan, J.-H. Tian, Y. Qiao, H. Wang, S.-H. Luo, Z.-D. Meng, B.-W. Mao, J.-F. Li, B. Ren, J. Aizpurua, V. A. Apkarian, P. N. Bartlett, J. Baumberg, S. E. J. Bell, A. G. Brolo, L. E. Brus, J. Choo, L. Cui, V. Deckert, K. F. Domke, Z.-C. Dong, S. Duan, K. Faulds, R. Frontiera, N. Halas, C. Haynes, T. Itoh, J. Kneipp, K. Kneipp, E. C. Le Ru, Z.-P. Li, X. Y. Ling, J. Lipkowsky, L. M. Liz-Marz  n, J.-M. Nam, S. Nie, P. Nordlander, Y. Ozaki, R. Panneerselvam, J. Popp, A. E. Russell, S. Schl  cker, Y. Tian, L. Tong, H. Xu, Y. Xu, L. Yang, J. Yao, J. Zhang, Y. Zhang, Y. Zhang, B. Zhao, R. Zenobi, G. C. Schatz, D. Graham, and Z.-Q. Tian, *Chem. Soc. Rev.* **54**(3), 1453 (2025).
- ¹⁶J.-F. Li, C.-Y. Li, and R. F. Aroca, *Chem. Soc. Rev.* **46**(13), 3962 (2017).
- ¹⁷P. L. Stiles, J. A. Dieringer, N. C. Shah, and R. P. Van Duyne, *Annu. Rev. Anal. Chem.* **1**, 601 (2008).
- ¹⁸D. Wei, S. Chen, and Q. Liu, *Appl. Spectrosc. Rev.* **50**(5), 387 (2015); P. Johansson, H. Xu, and M. K  ll, *Phys. Rev. B* **72**(3), 035427 (2005).
- ¹⁹G. Barbillon, *Nanoplasmonics: Fundamentals and Applications* (BoD – Books on Demand, 2017), p. 496.
- ²⁰H. Yu, Y. Peng, Y. Yang, and Z.-Y. Li, *npj Comput Mater.* **5**(1), 1 (2019).
- ²¹J. R. Lakowicz, *Plasmonics* **1**(1), 5 (2006); J. R. Lakowicz, K. Ray, M. Chowdhury, H. Szmacinski, Y. Fu, J. Zhang, and K. Nowaczyk, *Analyst* **133**(10), 1308 (2008).
- ²²S. Bhaskar, L. Liu, W. Liu, J. Tibbs, L. D. Akin, A. Bacon, and B. T. Cunningham, *APL Mater.* **13**(4), 041103 (2025).
- ²³S. Bhaskar, L. Liu, W. Liu, J. Tibbs, and B. T. Cunningham, *MRS Bull.* **50**, 585–598 (2025).
- ²⁴A. Pokhriyal, M. Lu, V. Chaudhery, S. George, and B. T. Cunningham, *Appl. Phys. Lett.* **102**(22), 221114 (2013); P. C. Mathias, H.-Y. Wu, and B. T. Cunningham, *Appl. Phys. Lett.* **95**(2), 021111 (2009).
- ²⁵S.-H. Cao, W.-P. Cai, Q. Liu, and Y.-Q. Li, *Annu. Rev. Anal. Chem.* **5**(1), 317 (2012); M. Gharib, A. J. Yates, S. Sanders, J. Gebauer, S. Graf, A. R. Ziefu  , Nonappa, G. Kassier, C. Rehbock, S. Barcikowski, H. Weller, A. Alabastri, P. Nordlander, W. J. Parak, and I. Chakraborty, *Adv. Opt. Mater.* **12**(14), 2302833 (2024).
- ²⁶S. Bhaskar, A. K. Singh, P. Das, P. Jana, S. Kanvah, B. N. Bhaktha, and S. S. Ramamurthy, *ACS Appl. Mater. Interfaces* **12**(30), 34323 (2020); S. M. Lis, S. Bhaskar, R. Dahiwadkar, S. Kanvah, S. S. Ramamurthy, and B. N. Bhaktha, *ACS Appl. Nano Mater.* **6**(20), 19312 (2023); S. Bhaskar, P. Das, V. Srinivasan, B. N. Bhaktha, and S. S. Ramamurthy, *J. Phys. Chem. C* **124**(13), 7341 (2020).
- ²⁷S. D. Choudhury, R. Badugu, and J. R. Lakowicz, *Acc. Chem. Res.* **48**(8), 2171 (2015).
- ²⁸A. Rai, S. Bhaskar, P. Battampara, N. Reddy, and S. S. Ramamurthy, *Mater. Lett.* **316**, 132025 (2022); A. Rai, S. Bhaskar, K. M. Ganesh, and S. S. Ramamurthy, *Mater. Chem. Phys.* **285**, 126129 (2022).
- ²⁹A. Rai, S. Bhaskar, K. M. Ganesh, and S. S. Ramamurthy, *ACS Appl. Nano Mater.* **5**(9), 12245 (2022); M. H. Chowdhury, K. Ray, C. D. Geddes, and J. R. Lakowicz, *Chem. Phys. Lett.* **452**(1), 162 (2008).
- ³⁰S. S. Kharintsev, G. G. Hoffmann, A. I. Fishman, and M. K. Salakhov, *J. Phys. D: Appl. Phys.* **46**(14), 145501 (2013); S. Bhaskar, D. Thacharakkal, S. S. Ramamurthy, and C. Subramaniam, *ACS Sustainable Chem. Eng.* **11**(1), 78–91 (2023).
- ³¹Z. Li, *Adv. Opt. Mater.* **6**(16), 1701097 (2018).
- ³²P. Barya, Y. Xiong, S. Shepherd, R. Gupta, L. D. Akin, J. Tibbs, H. Lee, S. Singamaneni, and B. T. Cunningham, *Small* **19**, 2207239 (2023); W. Chen, K. D. Long, H. Yu, Y. Tan, J. S. Choi, B. A. Harley, and B. T. Cunningham, *Analyst* **139**(22), 5954 (2014); N. Ganesh, I. D. Block, P. C. Mathias, W. Zhang, E. Chow, and B. T. Cunningham, presented at the LEOS 2008 - 21st Annual Meeting of the IEEE Lasers and Electro-Optics Society, 2008; N. Ganesh, I. D. Block, P. C. Mathias, W. Zhang, E. Chow, V. Malyarchuk, and B. T. Cunningham, *Opt. Express* **16**(26), 21626 (2008).
- ³³B. Deng, Y. Zhang, G. Qiu, J. Li, L. L. Lin, and J. Ye, *Small* **20**(40), 2402235 (2024); C. S. Tye, A. Kufcs  k, C. A. Ross, K. Ehrlich, R. K. Henderson, and M. G. Tanner, *Biomed. Opt. Express* **16**(7), 2824 (2025).